# Torque Ripple Minimization of Four-phase Switched Reluctance Motor using Direct Torque Control with an Innovative Switching Sequence Scheme

Krishna Reddy Pittam†, Deepak Ronanki‡, Parthiban Perumal†, Abdul R. Beig§, and Sheldon S. Williamson‡
† Dept. of Electrical and Electronics Engineering, National Institute of Technology Karnataka, Surathkal 575 025, India
‡ Dept. of Electrical and Computer Engineering, University of Ontario Institute of Technology, Ontario L1G 0C5, Canada
§ Advanced Power and Energy Center, Dept. of Electrical and Computer Engineering, Khalifa University, Abu Dhabi, UAE
Email: krishnareddy4308@gmail.com, dronanki@ieee.org, and parthiban@nitk.edu.in,
balanthi.beig@ku.ac.ae and sheldon.williamson@uoit.ca

***Abstract*—Direct torque control (DTC) technique is the prominent control strategy, used to control the switched reluctance motor (SRM) with a reduced torque ripple in comparison to the traditional current control techniques. However, it draws higher phase current in order to maintain the required electromagnetic torque during phase commutation, thus reduces torque per ampere. To circumvent this issue, a new DTC method with an innovative switching sequence is introduced in this paper, which minimizes torque ripple as well as power loss. The efficacy of the proposed scheme is validated for four-phase SRM through detailed simulation studies and compared with the conventional DTC scheme. The results show that the proposed scheme exhibits an improved steady-state as well as dynamic performance under various operating conditions.**

***Index Terms*—Motor drives, switched reluctance motor, torque control, traction motors and torque ripple minimization.**

## I. Introduction

Energy crisis and greenhouse gas (GHG) emissions caused by fossil-fuel based vehicles lead to the advancements of the electric vehicle lead to nurture the electric vehicle (EV) technologies. In EVs, electric machines form a main energy conversion system and plays a vital impact on fuel consumption, driving range and comfort [1], [2]. Currently, permanent magnet synchronous motors (PMSMs) are widely used in electric power trains and are most dominant in the automotive industry. For instance, PMSMs with high-energy rare-earth permanent magnets of 80 kW and 105 kW are employed in the most popular EVs such as Nissan Leaf and Chevrolet Spark respectively [3], [4]. However, price volatility and the sensitivity of rare-earth magnets to temperature motivate researchers to develop magnet-free motor drive topologies that are more reliable and efficient [5].

Switched reluctance motors (SRMs) are one of the magnet-free motors, which are continuously capturing attention in automotive and industrial applications due to the distinctive features of robust structure, high starting torque with low starting current, low manufacturing cost, sustained for high rotational speeds and high temperatures [6]. However, it has shortcomings such as severe torque ripple, acoustic noise and vibration. Furthermore, a smooth torque control is strenuous due to non-linear, time-varying and strong coupling characteristics [7]. Therefore, research investigations are being actively performed to reduce torque ripple in the SRM drives.

Over the past years, many researchers have mainly focused on two aspects: the machine design and control strategy. Torque ripple minimization through machine design involves optimizing machine structure and parameters, the multi-phase machines and employing advanced multi-objective optimization [8]–[11]. It is well-known that higher phase SRMs generate reduced torque ripple and enhanced fault-tolerance in comparison to three-phase SRMs. For example, torque ripple in the three-phase SRMs is 20% more than four-phase SRMs. With continual improvements in packaging, digital controllers and power switching devices, the current research trend is more aligned towards the high-phase machines. However, use of asymmetric half-bridge converter (AHB) for higher phase machines increases the device count, thereby complicating the control algorithms and increasing the system cost [12]. In most of the applications the phase number of SRMs are limited to four and therefore four-phase SRMs are widely used [13].

On the other hand, minimization of the torque ripple can be achieved through optimising the control strategy including current profiling techniques [14], [15] and torque sharing functions [16], [17]. Alternatively, smooth torque control is achieved through direct average torque control (DATC) [18], direct instantaneous torque control (DITC) [19], direct torque and flux control (DTC) [20], [21] and model predictive control strategies [22]. The performance study among the aforementioned control strategies are studied and their comparison is presented in [23]–[25]. Among them, the DTC scheme [20] gained significant interest which adopts the principle of direct torque control (DTC) applied to traditional AC machines. This approach betrays faster dynamic response, reduced acoustic noise and does not require commutation angle control as well as rotor position information [24], [25]. Nonetheless, the active phase is must compensate negative torque engendered by the outgoing phase under the negative inductance slope region in order to retain the desired torque value. Thus, drawing more current from the source. As a result, net torque per ampere

978-1-7281-0395-2/19/$31.00 ©2019 IEEE

(T/A) is reduced, thereby lowering the SRM drive efficiency [26].

This paper presents a novel DTC scheme for four-phase SRM to improve T/A ratio while minimizing the torque ripple. In this method, a new switching sequence is developed based on the sixteen sector partition and the optimized voltage vectors are modified to eliminate negative torque initiated by the outgoing phase during a negative inductance slope. To verify the effectiveness of the proposed DTC scheme, detailed simulation studies have been carried out using MATLAB/SIMULINK. The performance of the proposed DTC scheme is validated on both steady-state as well as dynamic conditions and compared with the conventional DTC scheme.

## II. Modeling and Power Converter of an SRM

The SRM is a doubly salient machine and highly non-linear machine, which makes it difficult to control. Therefore, it is requisite to build the dynamic model of the SRM drive based on the non-linear model of SRM, which can be represented with a set of electrical equations and the system dynamics. According to fundamental circuit laws, the voltage equation of $q$-phase SRM is expressed as

$$\left.\begin{aligned} v_j &= r_j \cdot i_j + \frac{d\psi_j(i_j,\theta_j)}{dt}; j \;=\; 1, 2 \ldots\ldots\; q \\ v_j &= r_j \cdot i_j + \frac{\partial \psi_j}{\partial i_j} \cdot \frac{di_j}{dt} + \frac{\partial \psi_j}{\partial \theta_j} \cdot \frac{d\theta_j}{dt} \end{aligned}\right\} \quad (1)$$

The dynamic equation of the phase current neglecting mutual inductance can be expressed as

$$\frac{di_j}{dt} = \left[\frac{\partial \psi_j}{\partial i_j}\right]^{-1} \cdot \left[v_j - r_j \cdot i_j - \frac{\partial \psi_j}{\partial \theta_j} \cdot \omega\right]; \omega = \frac{d\theta}{dt} \quad (2)$$

where $v_j$, $r_j$, $i_j$, $\theta_j$, $\psi_j$ represents terminal voltage, phase winding resistance, phase current, rotor position and flux linkages "$q$"-phase respectively.

From the principle of the electromechanical energy conversion, the instantaneous electromagnetic torque at any rotor position is given by

$$T_m = \left.\frac{\partial W_c(i_j,\theta)}{\partial \theta}\right|_{i_j = constant} \quad (3)$$

where $W_c(i_j,\theta)$ denotes co-energy, which can be given by

$$W_c = \int_0^i \psi(i,\theta) \cdot di = \int_0^i L(i,\theta) \cdot i \cdot di \quad (4)$$

The dynamic equations of the mechanical system is expressed as

$$\frac{d\omega}{dt} = \frac{1}{J}\left[\sum_{j=1}^{q} T_j(i_j,\theta_j) - T_L - B \cdot \omega\right] \quad (5)$$

To study the high performance control techniques, a non-linear model of an SRM is developed using electromagnetic (flux and torque) characteristics [27]. Several inverter circuits to control SRM with unipolar current are presented in [28]. Among them, asymmetric H-bridge converter (AHB) has gained attention as it provides flexibility in controlling each phase independently. Fig. 1 shows the per-phase schematic

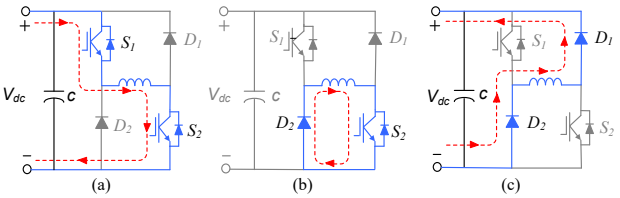


Fig. 1: Per-phase circuit of AHB converter.

TABLE I: Switching states of AHB converter

| $S_1$ | $S_2$ | $D_1$ | $D_2$ | *State* |
|---|---|---|---|---|
| 1 | 1 | 0 | 0 | Magnetizing state (+1) |
| 1 | 0 | 1 | 0 | Freewheeling state (0) |
| 0 | 1 | 0 | 1 | Freewheeling state (0) |
| 0 | 0 | 1 | 1 | Demagnetizing state (-1) |

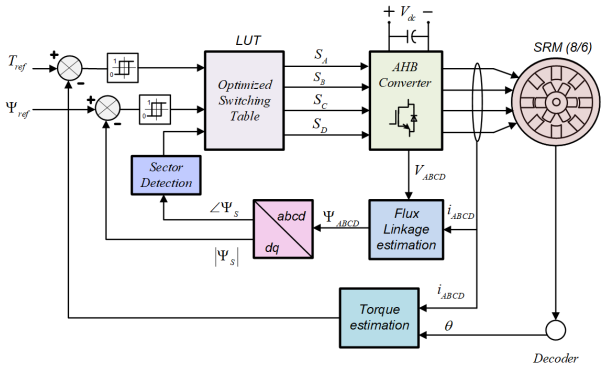


Fig. 2: Block diagram of DTC strategy of the four-phase SRM.

representation of AHB converter and three possible states that can be achieved to drive the SRM are listed in Table I.

TABLE II: Switching sequence for the eight sector partition method using the conventional DTC strategy

| **Sector** ($N_k$) | $T \Uparrow \psi \Uparrow$ | $T \Uparrow \psi \Downarrow$ | $T \Downarrow \psi \Uparrow$ | $T \Downarrow \psi \Downarrow$ |
|---|---|---|---|---|
| $N_1$ | $V_2$ | $V_4$ | $V_8$ | $V_6$ |
| $N_2$ | $V_3$ | $V_5$ | $V_1$ | $V_7$ |
| $N_3$ | $V_4$ | $V_6$ | $V_2$ | $V_8$ |
| $N_4$ | $V_5$ | $V_7$ | $V_3$ | $V_1$ |
| $N_5$ | $V_6$ | $V_8$ | $V_4$ | $V_2$ |
| $N_6$ | $V_7$ | $V_1$ | $V_5$ | $V_3$ |
| $N_7$ | $V_8$ | $V_2$ | $V_6$ | $V_4$ |
| $N_8$ | $V_1$ | $V_3$ | $V_7$ | $V_5$ |

## III. Proposed DTC Scheme

The DTC of an SRM adopts the philosophy of controlling the torque of AC machines [20]. The control block diagram of an SRM using the DTC scheme is shown in Fig. 2. This scheme comprises of hysteresis-based torque, flux comparators, a flux-linkage vector's position information and switching table to generate optimal voltage vectors to the control magnitude of stator flux linkage and electro-magnetic torque. In this method, the total electrical space is divided

TABLE III: Switching sequence for the sixteen sector partition method using the proposed DTC strategy

| **Sector** ($N_k$) | $T \Uparrow \psi \Uparrow$ | $T \Uparrow \psi \Downarrow$ | $T \Downarrow \psi \Uparrow$ | $T \Downarrow \psi \Downarrow$ |
|---|---|---|---|---|
| $N_1$ | $V_2$ | $V_3$ | $V_{10}$ | $V_9$ |
| $N_2$ | $V_3$ | $V_4$ | $V_{11}$ | $V_{10}$ |
| $N_3$ | $V_3$ | $V_4$ | $V_{11}$ | $V_{10}$ |
| $N_4$ | $V_4$ | $V_5$ | $V_{12}$ | $V_{11}$ |
| $N_5$ | $V_4$ | $V_5$ | $V_{12}$ | $V_{11}$ |
| $N_6$ | $V_5$ | $V_6$ | $V_{13}$ | $V_{12}$ |
| $N_7$ | $V_5$ | $V_6$ | $V_{13}$ | $V_{12}$ |
| $N_8$ | $V_6$ | $V_7$ | $V_{14}$ | $V_{13}$ |
| $N_9$ | $V_6$ | $V_7$ | $V_{14}$ | $V_{13}$ |
| $N_{10}$ | $V_7$ | $V_8$ | $V_{15}$ | $V_{14}$ |
| $N_{11}$ | $V_7$ | $V_8$ | $V_{15}$ | $V_{14}$ |
| $N_{12}$ | $V_8$ | $V_1$ | $V_{16}$ | $V_{15}$ |
| $N_{13}$ | $V_8$ | $V_1$ | $V_{16}$ | $V_{15}$ |
| $N_{14}$ | $V_1$ | $V_2$ | $V_9$ | $V_{16}$ |
| $N_{15}$ | $V_1$ | $V_2$ | $V_9$ | $V_{16}$ |
| $N_{16}$ | $V_2$ | $V_3$ | $V_{10}$ | $V_9$ |

into eight sectors with an angle of $45^o$. This scheme selects a switching sequence as per Table II and selects the suitable voltage vector to reduce torque and flux errors. However, due to the extension of phase current into negative torque region in the conventional DTC scheme results in high torque pulsations and lowering the efficiency of an SRM drive, which is unenviable feature of a motor drive in vehicular applications. The low T/A of the machine is due to the magnetization of any phase during negative inductance slope region that results in the production of negative torque. In order to recompense this negative torque produced by outgoing phase during negative torque region, the active phase has to produce more positive torque thereby drawing more current from the dc-source.

To address this issue, a new switching sequence is developed that eliminates the transition from demagnetization to magnetization of all phases, thereby minimizes torque ripple along with enhanced T/A ratio. In this study, new vector selection rules are proposed for increasing torque and decreasing torque which can be controlled independently. To realize the optimal switching sequence, sixteen sector partition method with an electrical angle of $22.5^o$ is employed [26] and each sector $N_k$ ($k \in \{1, 2, ...., 16\}$ ) covers only $22.5^o$. The sixteen sector partition approach allows the precise selection of voltage vectors corresponding to torque and flux errors. Furthermore, the proposed strategy also achieves fast dynamic response by choosing a vector which is at right angles (+90$^o$ and -90$^o$) to the flux linkage vector for increasing ($T\Uparrow$) or decreasing ($T\Downarrow$) torque. The switching sequence for sector I ($N_1$) of sixteen sectors for increasing ($T\Uparrow$) and decreasing ($T\Downarrow$) are shown in Fig. 3(a) and (b) respectively. The switching sequence for all the sectors using the proposed DTC strategy is listed in Table III. The proposed method effectively improves T/A and reduces torque pulsation by replacing magnetization of any phase during negative torque region with demagnetization/freewheeling of the active phase.

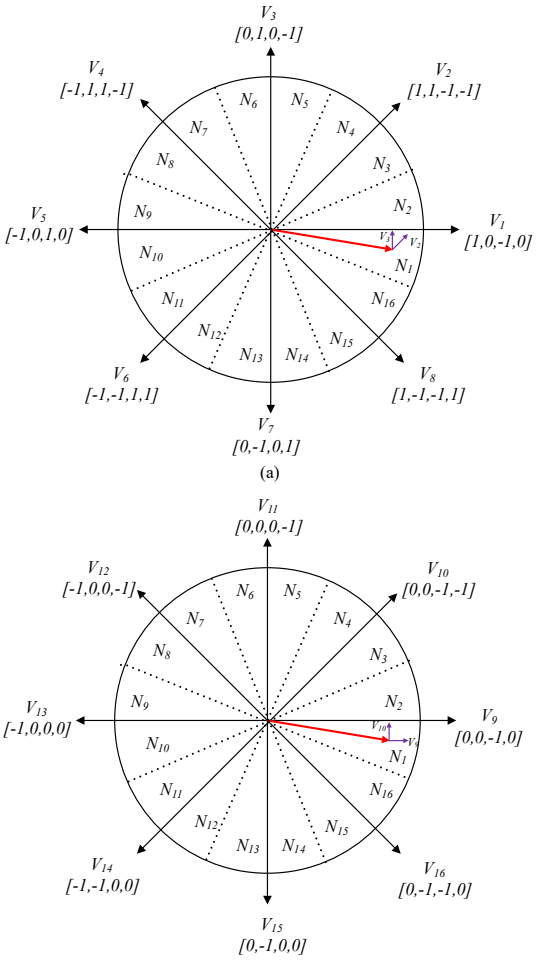


Fig. 3: Voltage vector selection for sector $N_1$ using the proposed DTC scheme for (a) ($\Uparrow T$) (b) ($\Downarrow T$).

## IV. Simulation Results and Analysis

The simulation model of a four-phase SRM is implemented in MATLAB/Simulink to validate the performance and effectiveness of the proposed DTC scheme. In this study, a non-linear dynamic model is developed using magnetization and torque characteristics are obtained from experimental measurements on a 4 kW machine. The proposed control scheme is compared to the conventional DTC scheme described in [20], [21]. The simulation results of an SRM using the conventional DTC at 300 rpm and 800 rpm are shown in Fig. 4 and 5 respectively. It is observed that an individual phase conducts for a longer period due to automatic commutation angle control. As a result, phase current extends into negative inductive slope region, thereby negative phase torque. In other words, active phase has to generate more torque to compensate the negative torque generated by the outgoing phase at both low and high speeds. The rms value of the phase current required at all rotor positions is significantly high, thereby lowering the SRM drive efficiency besides the torque ripple.

To surmount the aforementioned issues, a novel DTC

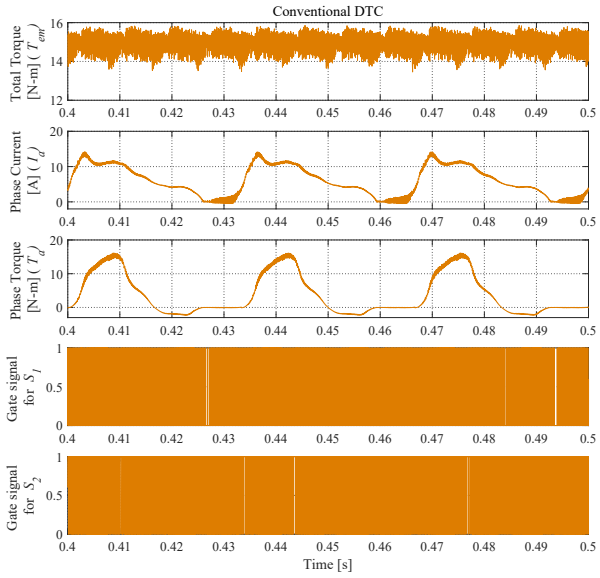


Fig. 4: Steady-state simulation results of an SRM drive at 300 rpm using the conventional DTC scheme.

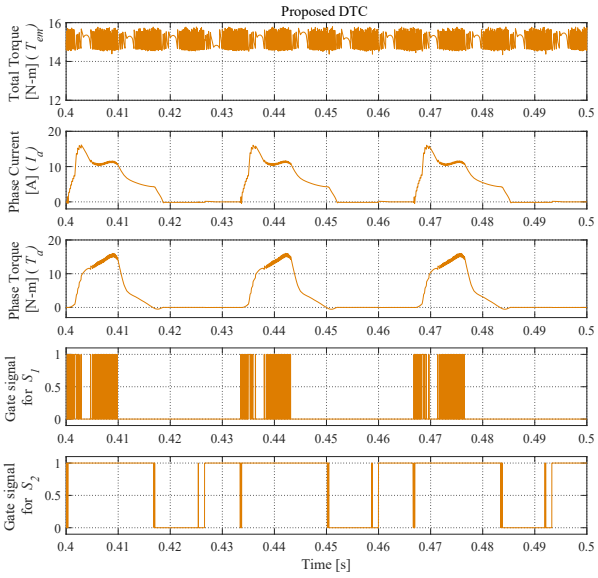


Fig. 6: Steady-state simulation results of an SRM drive at 300 rpm using the proposed DTC scheme.

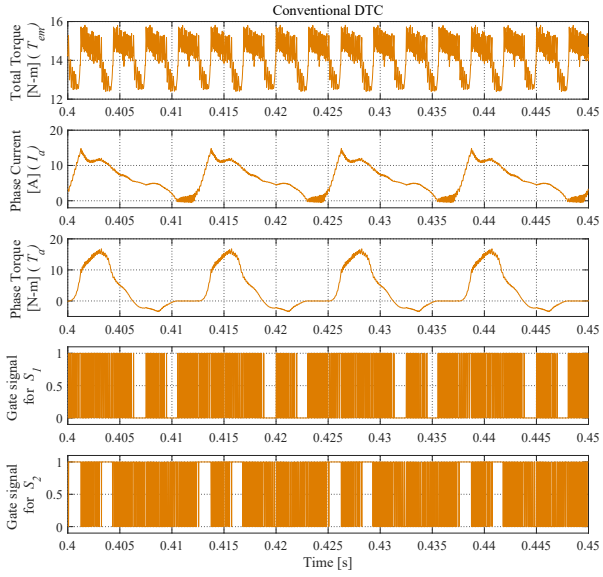


Fig. 5: Steady-state simulation results of an SRM drive at 800 rpm using the conventional DTC scheme.

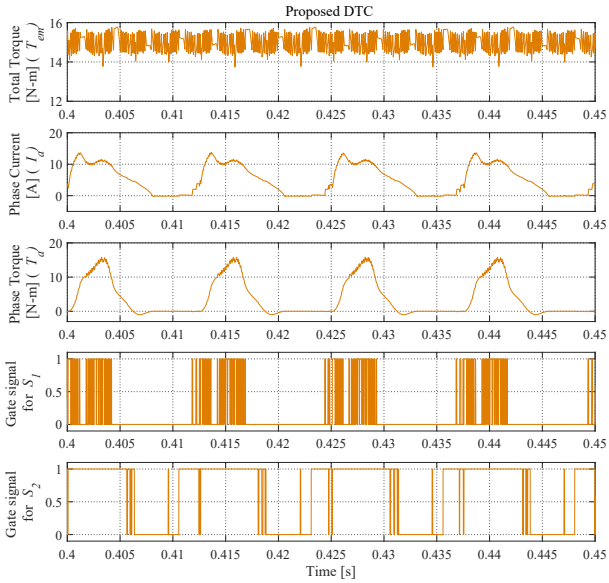


Fig. 7: Steady-state simulation results of an SRM drive at 800 rpm using the proposed DTC scheme.

strategy is proposed, which minimizes the torque ripple at all speeds while enhancing the torque/ampere ratio. The simulation waveforms of an SRM drive using the proposed DTC scheme at 300 rpm and 800 rpm are shown in Fig. 6 and 7 respectively. It is noticed that the torque ripple is significantly minimized at these speeds using the proposed DTC scheme. Moreover, the proposed scheme reduces the number of commutations as observed in gating signals for the switches, thereby allowing operation at a lower switching frequency. This implies that the number of switchings as well as device voltage stress are less in the proposed DTC strategy in comparison to the conventional DTC during each fundamental cycle. Therefore, the efficiency and reliability of the SRM drive is significantly improved.

Furthermore, the performance of the proposed DTC scheme is also verified under transient conditions such as step change

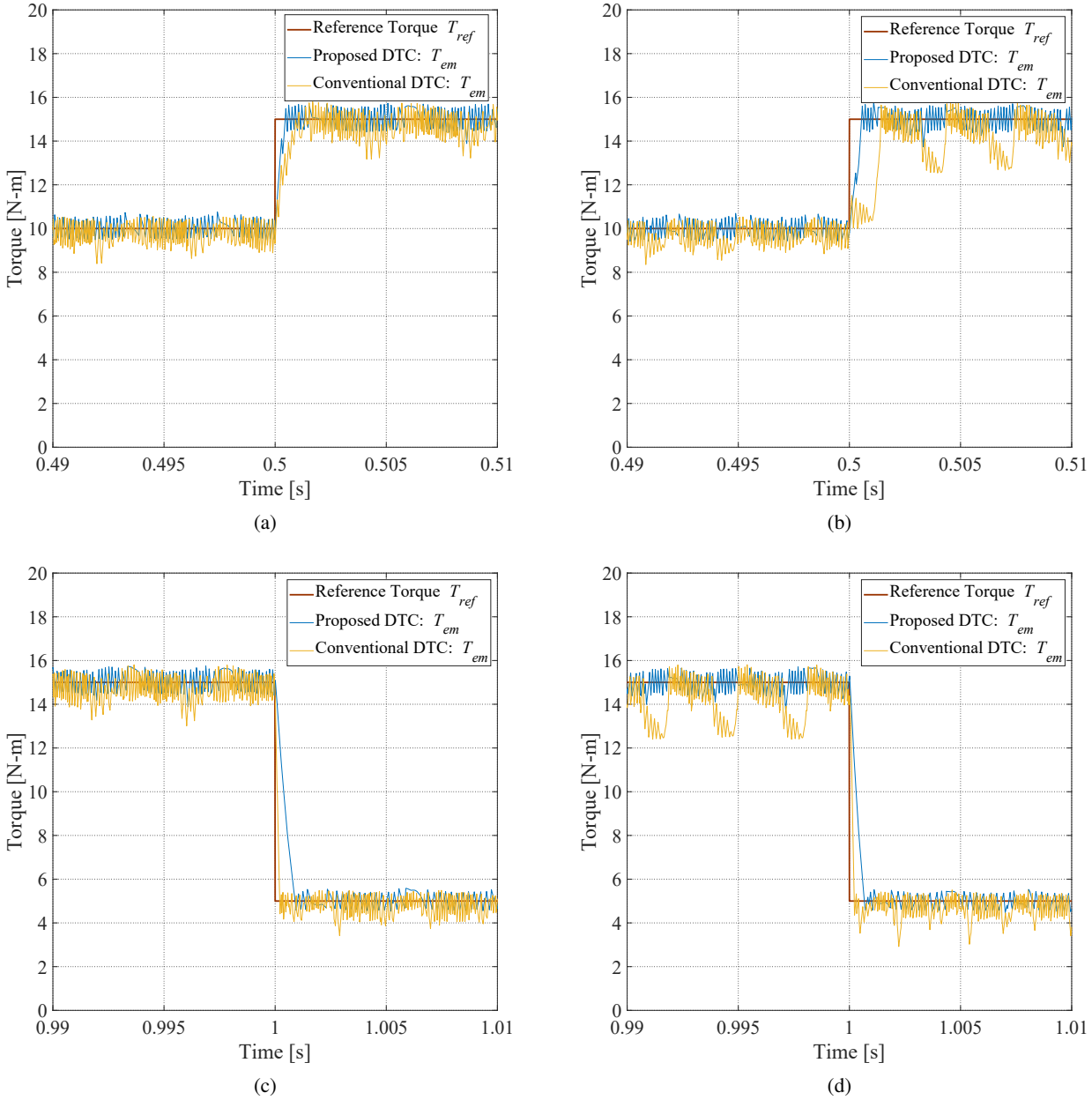


Fig. 8: Dynamic response of an SRM drive under step change in torque reference. (a) $T\uparrow$ at 600 rpm; (b) $T\uparrow$ at 800 rpm; (c) $T\downarrow$ at 600 rpm; and (d) $T\downarrow$ at 800 rpm.

in the torque reference both in acceleration and deceleration cases. The results of the SRM drive using the proposed DTC strategy in comparison to the conventional under the both cases are shown in Fig. 8. It is noticed that the proposed DTC scheme shows faster dynamic response in comparison to the conventional DTC scheme. It is known that flux vector information in the DTC scheme with some correction factor is enough for the sensorless operation. The proposed scheme also helps to minimize the prediction error due to employment of the sixteen sector partition method. The performance comparison of both these control strategies at different speeds is presented in Table IV. It can be concluded that torque of an SRM is well controlled at their reference value using the proposed DTC method and overwhelms the conventional DTC scheme in minimizing the torque ripple and enhancing the T/A ratio.

## V. Conclusion

This paper proposes a new DTC strategy for a four-phase SRM with an innovative switching sequence to enhance torque per ampere ratio and reduces torque ripple. In this scheme, a

TABLE IV: Performance comparison between the proposed DTC and the conventional DTC

| **Speed (rpm)** | **Conventional DTC Scheme** | | | | **Proposed DTC Scheme** | | | |
|---|---|---|---|---|---|---|---|---|
| | $T_{rms}$ [N-m] | $I_s$ [A] (rms) | T/A (rms) | $T_{ripple}$ [N-m] | $T_{rms}$ [N-m] | $I_s$ [A] (rms) | T/A (rms) | $T_{ripple}$ [N-m] |
| 300 | 14.82 | 9.517 | 1.557 | 14.66 | 15.12 | 5.947 | 2.542 | 09.21 |
| 400 | 14.77 | 9.403 | 1.570 | 17.33 | 15.09 | 6.608 | 2.283 | 10.01 |
| 500 | 14.72 | 9.627 | 1.529 | 19.01 | 15.04 | 7.311 | 2.057 | 13.01 |
| 600 | 14.69 | 9.652 | 1.521 | 18.60 | 15.10 | 8.032 | 1.879 | 13.33 |
| 700 | 14.59 | 9.467 | 1.541 | 22.01 | 15.01 | 8.770 | 1.711 | 13.61 |
| 800 | 14.18 | 9.386 | 1.510 | 22.66 | 15.02 | 9.493 | 1.582 | 13.61 |

sixteen sector partition scheme is employed and a switching sequence is selected to eliminate the instantaneous negative torque generated during the phase commutation. Thus, it enhances the torque per ampere, thereby improving the efficiency of the traction drive. The results show the improved performance of SRM drive using the proposed DTC scheme in comparison to the conventional DTC strategy.

## REFERENCES


[1] B. Bilgin *et al.*, "Making the Case for Electrified Transportation," *IEEE Trans. Transport. Electrific.*, vol. 1, no. 1, pp. 4-17, June 2015.

[2] D. Ronanki and P. Perumal, "A Small 4-wheeler EV Propulsion System Using DTC Controlled Induction Motor," in *Proc. World Congress on Engineering*, vol. 2, London, UK, July 2013.

[3] Y. Sato, S. Ishikawa, T. Okubo, M. Abe, and K. Tamai, "Development of high response motor and inverter system for the Nissan Leaf electric vehicle," *SAE Technical Paper*, 2011-01-0350, 2011.

[4] F. Momen, K. Rahman and Y. Son, "Electrical Propulsion System Design of Chevrolet Bolt Battery Electric Vehicle," *IEEE Trans. Ind. Appl.*, vol. 55, no. 1, pp. 376-384, Jan.-Feb. 2019.

[5] I. Boldea, L. N. Tutelea, L. Parsa and D. Dorrell, "Automotive Electric Propulsion Systems With Reduced or No Permanent Magnets: An Overview," *IEEE Trans. Ind. Electron.*, vol. 61, no. 10, pp. 5696-5711, Oct. 2014.

[6] Z. Yang, F. Shang, I. P. Brown and M. Krishnamurthy, "Comparative Study of Interior Permanent Magnet, Induction, and Switched Reluctance Motor Drives for EV and HEV Applications," *IEEE Trans. Transport. Electrific.*, vol. 1, no. 3, pp. 245-254, Oct. 2015.

[7] E. Bostanci, M. Moallem, A. Parsapour and B. Fahimi, "Opportunities and Challenges of Switched Reluctance Motor Drives for Electric Propulsion: A Comparative Study," *IEEE Trans. Transport. Electrific.*, vol. 3, no. 1, pp. 58-75, March 2017.

[8] Y. K. Choi, H. S. Yoon and C. S. Koh, "Pole-Shape Optimization of a Switched-Reluctance Motor for Torque Ripple Reduction," *IEEE Trans. Magn.*, vol. 43, no. 4, pp. 1797-1800, April 2007.

[9] S. I. Nabeta, I. E. Chabu, L. Lebensztajn, D. A. P. Correa, W. M. da Silva and K. Hameyer, "Mitigation of the Torque Ripple of a Switched Reluctance Motor Through a Multiobjective Optimization," *IEEE Trans. Magn.*, vol. 44, no. 6, pp. 1018-1021, June 2008.

[10] V. Rallabandi and B. G. Fernandes, "Design Methodology for High-Performance Segmented Rotor Switched Reluctance Motors," *IEEE Trans. Energy Convers.*, vol. 30, no. 1, pp. 11-21, March 2015.

[11] C. Ma and L. Qu, "Multiobjective Optimization of Switched Reluctance Motors Based on Design of Experiments and Particle Swarm Optimization," *IEEE Trans. Energy Convers.*, vol. 30, no. 3, pp. 1144-1153, Sept. 2015.

[12] S. Xu, H. Chen, F. Dong and J. Yang, "Design and Development of Low Torque Ripple Variable-Speed Drive System With Six-Phase Switched Reluctance Motors," *IEEE Trans. Energy Convers.*, vol. 33, no. 1, pp. 420-429, March 2018.

[13] S. Xu, H. Chen, F. Dong and J. Yang, "Reliability Analysis on Power Converter of Switched Reluctance Machine System under Different Control Strategies," *IEEE Trans. Ind. Electron.*, vol. 66, no. 8, pp. 6570-6580, Aug. 2019.

[14] J. Y. Chai and C. M. Liaw, "Reduction of speed ripple and vibration for switched reluctance motor drive via intelligent current profiling," *IET Electric Power Appli.*, vol. 4, no. 5, pp. 380-396, May 2010.

[15] R. Mikail, I. Husain, Y. Sozer, M. S. Islam and T. Sebastian, "Torque-Ripple Minimization of Switched Reluctance Machines Through Current Profiling," *IEEE Trans. Ind. Appl.*, vol. 49, no. 3, pp. 1258-1267, May-June 2013.

[16] X. D. Xue, K. W. E. Cheng and S. L. Ho, "Optimization and Evaluation of Torque-Sharing Functions for Torque Ripple Minimization in Switched Reluctance Motor Drives," *IEEE Trans. Power Electron.*, vol. 24, no. 9, pp. 2076-2090, Sept. 2009.

[17] H. Li, B. Bilgin and A. Emadi, "An Improved Torque Sharing Function for Torque Ripple Reduction in Switched Reluctance Machines," *IEEE Trans. Energy Convers.*, vol. 34, no. 2, pp. 1635-1644, Feb. 2019.

[18] R. B. Inderka and R. W. A. A. De Doncker, "High-dynamic direct average torque control for switched reluctance drives," *IEEE Trans. Ind. Appl.*, vol. 39, no. 4, pp. 1040-1045, July-Aug. 2003.

[19] R. B. Inderka and R. W. A. A. De Doncker, "DITC-direct instantaneous torque control of switched reluctance drives," *IEEE Trans. Ind. Appl.*, vol. 39, no. 4, pp. 1046-1051, July-Aug. 2003.

[20] A. D. Cheok and Y. Fukuda, "A new torque and flux control method for switched reluctance motor drives," *IEEE Trans. Power Electron.*, vol. 17, no. 4, pp. 543-557, July 2002.

[21] D. Ronanki and P. Parthiban, "PV-Battery Powered Direct Torque Controlled Switched Reluctance Motor Drive," in *Proc. IEEE Asia-Pacific Power and Energy Eng. Conf.*, Shanghai, 2012, pp. 1-4.

[22] C. Li, G. Wang, Y. Li and A. Xu, "An improved finite-state predictive torque control for switched reluctance motor drive," *IET Electric Power Appl.*, vol. 12, no. 1, pp. 144-151, 2018.

[23] A. Pop, V. Petrus, C. S. Martis, V. Iancu and J. Gyselinck, "Comparative study of different torque sharing functions for losses minimization in Switched Reluctance Motors used in electric vehicles propulsion," in *Proc. IEEE Int. Conf. on Optimization of Electrical and Electronic Equipment (OPTIM)*, Brasov, 2012, pp. 356-365.

[24] D. Ronanki and S. S. Williamson, "Comparative analysis of DITC and DTFC of switched reluctance motor for EV applications," in *Proc. IEEE Int. Conf. on Ind. Tech. (ICIT)*, Toronto, ON, 2017, pp. 509-514.

[25] S. Sau, R. Vandana and B. G. Fernandes, "A new direct torque control method for switched reluctance motor with high torque/ampere," in *Proc. 39th Annu. Conf. of the IEEE Ind. Electron. Soc.*, Vienna, 2013, pp. 2518-2523.

[26] P. K. Reddy, D. Ronanki and P. Parthiban, "Direct torque and flux control of switched reluctance motor with enhanced torque per ampere ratio and torque ripple reduction," *Electronics Letters*, vol. 55, no. 8, pp. 477-478, 2019.

[27] P. Chancharoensook and M. F. Rahman, "Dynamic modeling of a four-phase 8/6 switched reluctance motor using current and torque look-up tables," in *Proc. 28th Annu. Conf. of the IEEE Ind. Electron. Soc.*, Sevilla, 2002, pp. 491-496.

[28] M. Pittermann, J. Fort, J. Diesl and V. Pavlicek, "Converters for Switched Reluctance Motor - Topology Comparison," in *Proc. Int. Conf. on Mechatronics - Mechatronika (ME)*, Brno, Czech Republic, 2018, pp. 1-8.